minerals

MDPI

Review

Effects of Steel Slag Powder as A Cementitious Material on Compressive Strength of Cement-Based Composite

Guohua Sheng *, Chao Li, Shengji Jin and Quan Bai

School of Architecture and Civil Engineering, Shenyang University of Technology, Shenyang 110870, China; 18749023798@163.com (C.L.); shengjijin@sut.edu.cn (S.J.); baiquan@163.com (Q.B.)
* Correspondence: sgh190@163.com; Tel.: +86-024-25496580

Abstract: The utilization rate of steel slag in China is far behind that of developed countries. The annual output of steel slag is still increasing, resulting in a large amount of accumulation, causing environmental pollution. This paper summarizes and analyzes the relevant research on steel slag powder (SSP) as a cementitious material, studies the effect of SSP replaces cement as single or multiple admixtures, with different specific surface areas, and the amount of activator on the compressive strength of cement-based material. The results show that due to the lower content of active substances in SSP compared to cement, the strengths decrease with the increase of the replacement ratio R, which is the ratio of SSP to cement. R = 30% is important for replacing cement with single SSP. When replacing cement with the mixture of SSP and slag/fly ash, the strengths of most groups decrease with the increase of the mix replacement ratio R_c. The decreasing trend is not obvious due to the pozzolanic effect. There is an optimal dosage for using a single activator to activate SSP. The effect of using multiple activators in combination is better than that of single one. The strength increases with the increase of the specific surface area (SSA) of SSP. However, if the SSA is too high, it will not only increase the preparation cost, but also reduce the increase in strength due to the agglomeration effect of SSP. The optimal range of specific surface area SSA is 400 m^2/kg~500 m^2/kg. With the increase of age t, the compressive strength increases. The effect of the curing methods on the compressive strength is hot and heat curing > standard curing > natural curing.

Keywords: steel slag powder; compressive strength; cementitious material; replacement ratio; specific surface area; activator

check for updates

Citation: Sheng, G.; Li, C.; Jin, S.; Bai, Q. Effects of Steel Slag Powder as A Cementitious Material on Compressive Strength of Cement-Based Composite. *Minerals* **2023**, *13*, 869. https://doi.org/10.3390/min13070869

Academic Editor: Elsabe Kearsley

Received: 23 May 2023
Revised: 16 June 2023
Accepted: 24 June 2023
Published: 28 June 2023

Copyright: © 2023 by the authors. Licensee MDPI, Basel, Switzerland. This article is an open access article distributed under the terms and conditions of the Creative Commons Attribution (CC BY) license (https://creativecommons.org/licenses/by/4.0/).

1. Introduction

Steel slag is the solid waste produced in the process of steelmaking, and the annual discharge is 15%~20% of the crude steel output [1–4]. From a worldwide perspective, the output of steel slag has surged from about 150~230 million tons in 2012 to 190~290 million tons in 2018, an increase of about 30% [5,6]. According to the "Guiding Opinions on Comprehensive Utilization of Bulk Solid Wastes in the Fourteenth Five-Year Plan" jointly issued by the National Development and Reform Commission in 2021, the accumulated storage of bulk solid waste is about 60 billion tons, and the annual added storage is close to 3 billion tons in China. It is explicitly pointed out that the utilization rate of steel slag is still low, resulting in the occupation of a large number of land resources and ecological and environmental security risks, and clearly requested to expand the utilization rate of steel slag in concrete materials [7].

The comprehensive utilization rate of steel slag in developed countries such as the United States and Japan is about 90% [8]. In Europe, it is also maintained at a high level [9,10]. It was not until the end of the 20th century that China began to study steel slag material, which also led to relatively backward technology and a low utilization rate [11,12]. However, with the improvement of scientific and technological level in recent years, the process level of iron removal from steel slag and reduction of f-CaO has been

further improved, and high-quality steel slag materials can be produced [13]. The use characteristics and methods of steel slag powder (SSP) as a cementitious material have been comprehensively understood [14–16].

Cement is a material with high productivity and high energy consumption [17]. By 2021, global cement production has reached 4.4 tons [18]. It has a huge impact on the environment. Producing 1 ton of cement will produce 0.7 tons of CO_2 [19]. For China, a developing country with a huge demand for cement, finding a new cementitious material to replace cement and manufacturing green building products has a huge application prospect [20].

Based on the above background, this paper summarizes and analyzes the research on SSP as a cementitious material and draws relevant conclusions on the effect of it on compressive strength of concrete, paste, mortar and the improvement of application problems. The content mainly involves the effect of SSP as a cementitious material replacing cement with single or multiple admixtures, with different specific surface areas (SSA), different excitation methods and the amount of activator on the compressive strength of cement-based composite. The effect of SSP on the compressive strength is further clarified, through the analysis of relevant literature data, and a summary of conclusions and the combination of chemical reaction formula is provided, laying a theoretical foundation for its wide application as a cementitious material.

2. Cementitious Properties of SSP

SSP can be used as a cementitious material by aging, grinding, iron removal and impurity reduction. Its main mineral phases include olivine, molybdenite, C_3S, β-C_2S, γ-C_2S, C_4AF, C_2F "RO" phase (CaO-FeO-MnO-MgO solid solution), *f*-CaO and *f*-MgO [21–27]. It also shows that the hydration process is similar to that of cement. During its production process, β-C_2S can be converted into γ-C_2S, along with the increase of volume, leads to crystal self-crushing into powder, which significantly reduces the grinding cost. A detailed introduction to the transformation process from β-C_2S into γ-C_2S was provided, and the optimal conditions in detail for self-disintegration of items and cooling rates were analyzed through differential thermal analysis (DTA) and calorimetry [28]. Although γ-C_2S is not hydraulic and has no significant contribution to the formation of cementitious materials, and the content of active substance such as C_3S β-C_2S, C_4AF, C_2F, etc., are less than those of cement, it is found that the content of them increase with the increase of alkalinity of SSP, providing weak cement properties [28,29].

According to the specifications of Steel Slag Powder for Cement and Concrete (GB/T 20491-2017), SSP is divided into Grade I and Grade II according to the activity index, the alkalinity coefficient is not less than 1.8, and the SSA is not less than 400 m^2/kg. The *M* coefficient proposed by Mason is calculated based on the chemical composition; the chemical composition range of SSP currently used in China is shown in Table 1 [30,31].

Table 1. Main chemical composition and range of steel slag powder (%).

CaO	SiO_2	Al_2O_3	FeO	Fe_2O_3	MgO
45~60	10~15	1~5	7~20	3~9	3~13

3. Effect of SSP on Compressive Strength

Collect and screen the test data of the experimental references and the principles of screening are as follows:

The test data include the control group, i.e., the replacement ratio $R = 0$.

The alkalinity of SSP are all larger than 1.8.

When comparing each group of test data, the mix proportions of other materials shall be the same except *R*.

The compressive strength of test specimens obtained by 28 days of standard curing from Sections 3.1–3.4.

3.1. Replacing Cement with SSP

Replacing cement with SSP in a certain ratio *R* of concrete, mortar, paste is the simplest way to reflect the effect on compressive strength. Based on the above principles, 29 references and 39 groups (different proportions) are summarized and analyzed. Table 2 is the key conclusions and compressive strength range of each reference.

Table 2. Summary of different replacement ratio *R* for cement-based composite.

Reference	*R* (%)	Strength (Mpa)	Type	Key Conclusions of Different Replacement Ratio *R*
Guo and Shi [32]	0~50	60~32	paste	With the increase of *R*, the strength decreases.
Muhmood et al. [a] [33].	0~30	66.5~53.4	paste	With the increase of *R*, the strength decreases.
Muhmood et al. [b] [33].	0~30	66.5~51.4		
Liu and Li [26]	0~45	57~37	mortar	With the increase of *R*, the strength decreases.
Saly et al. [a] [34]	0~45	48.7~31.5	mortar	The strengths are lower than that of the control group. The strength decreases linearly with the increase of *R*.
Saly et al. [b] [34]	0~45	48.7~35.9	mortar	The strengths are lower than that of the control group. When $R \geq$ 30%, they decrease rapidly.
Peng et al. [35]	0~47.1	113.1~87.8	mortar	All the strengths are lower than that of the control group. The optimal mixing ratio R = 30%.
Liu and Guo [36]	0~20	156~140	mortar	With the increase of *R*, the strength decreases, and the decrease rate is gradually increased.
Shi et al. [37]	0~50	53~56~36	mortar	The strength first increases and then decreases with the increase of *R*. The early hydration rate of SSP is lower than that of cement.
Zhang et al. [38]	0~40	44~16	mortar	With the increase of *R*, the strength decreases. When $R \geq$ 20%, the strength decreases rapidly.
Xu et al. [39]	0~40	54~44	mortar	The compressive strength decreases with the increase of *R*, but except R = 10%.
Gan et al. [a] [40]	0~10	37.65~31.25	mortar	With the increase of *R*, the strength decreases.
Zhang et al. [a] [41]	0, 63	51~34	mortar	With the increase of *R*, the strength decreases.
Altun and Yılmaz [a] [42]	0~45	58~35.7	mortar	With the increase of *R*, the compressive strength decreases linearly.
Altun and Yılmaz [b] [42]	0~45	58~43.7		
da Silva et al. [43].	0~20	55~53	mortar	When $R \leq$ 20%, SSP has little effect on strength.
Wang et al. [44]	0~40	48.3~28.1	mortar	With the increase of *R*, the strength decreases.
Wang et al. [a] [45]	0~60	54~27	mortar	With the increase of *R*, the strength decreases.
Wang et al. [b] [45]	0~60	60~35		
Wang [46]	0~50	37.9~21.4	concrete	When R = 20%, the strength is the highest but lower than the control group. When $R \geq$ 30%, the strength decreases rapidly.
Guan [a] [47]	0~50	65.1~47.9	concrete	With the increase of *R*, the strength decreases. When $R \geq$ 30%, the strength decreases rapidly.
Li [a] [48]	0~50	67.1~47.1	concrete	With the increase of *R*, the strength decreases When $R \geq$ 30%, the strength decreases rapidly.
Li [b] [48]	0~50	48.4~29.8	concrete	All the strengths are lower than that of the control group. The optimal mixing ratio R = 20%~30%.
Li [c] [48]	0~50	65.8~38.2	concrete	All the strengths are lower than that of the control group. When R = 20%~50%, the strength decreases significantly with the increase of *R*.
Li [d] [48]	0~50	44.7~26.7	concrete	All the strengths are lower than that of the control group. When R = 30%~50%, the strength decreases significantly with the increase of *R*.
Cai [a] [49]	0~50	40~44~28	concrete	When $0 < R \leq$ 30%, the strengths are higher than that of the control group, and when $R >$ 30%, the strengths are decrease.
Wang [50]	0~45	52~48~33	concrete	The strength decreases with the increase of *R*.
Ding et al. [51]	0~30	47~49.5~42	concrete	When $R \leq$ 20%, the strengths are higher than the control group. When R = 30% is lower than the base group.
Liu [a] [52]	0~45	60.1~60.5~49.2	concrete	When $R \leq$ 10%, the strengths are higher than that of the control group. When $R >$ 30%, the strengths decreases rapidly.
Liu [b] [52]	0~45	57.8~58.9~45.7		
Liu [c] [52]	0~45	43.4~47~34.9		
Luo et al. [53]	0~17.6	39.9~30.7	concrete	The strengths are lower than that of the control group. When $R \geq$ 10%, they decrease rapidly.
Sha et al. [54]	0~35	48~52.1~37	concrete	When $R \leq$ 15%, the strengths are higher than that of the control group. When $R \geq$ 25%, the strengths decreases.
Hussain et al. [55]	0~30	60.3~68.6~43.7	concrete	With the increase of *R*, the strength first increases and then decreases, and the highest strength is 68.6 MPa when R = 10%.
Tüfekçi et a1. [a] [23]	0~15	32.9~26.7	concrete	With the increase of *R*, the strength decreases, SSP A has greater effect on strength than B.
Tüfekçi et a1. [b] [23]	0~15	32.9~30.1		
Li et a1. [a] [56]	0~40	55~48	concrete	With the increase of *R*, the strength decreases.
Wang et a1. [a] [57]	0~30	54~51	concrete	With the increase of *R*, the strength decreases.
Wang et a1. [b] [57]	0~30	79~82~73	concrete	The strength first increases and then decreases with the increase of *R*. and the highest strength is 82 MPa when R = 10%
Wang et a1. [a] [58]	0~60	50~24	concrete	With the increase of *R*, the strength decreases.
Wang et a1. [b] [58]		69~46		
Wang et a1. [c] [58]		50~22		
Wang et a1. [d] [58]		69~45		
Wang et a1. [e] [58]		50~24		
Wang et a1. [f] [58]		69~46		

Table 2. *Cont.*

Reference	*R* (%)	Strength (Mpa)	Type	Key Conclusions of Different Replacement Ratio *R*
Wang et a1. [g] [58]		50~25		
Wang et a1. [h] [58]		69~46		
Wang et a1. [i] [58]		50~20		
Wang et a1. [j] [58]		69~41		
Song and Liu [59]	0~40	42.5~47~29	concrete	The strength first increases and then decreases with the increase of *R*. The highest strength is 47 MPa when *R* = 15.

Note: Superscripts a–j represents different mix proportion in each reference.

Except for reference [35] which conducted nine and reference [53] which conducted six reproducibility tests, all other references (groups) in Table 2 conducted three reproducibility tests.

The compressive strengths corresponding to replacement ratio *R* of all the references are shown in Figures 1 and 2. Although the control strength (*R* = 0) varies greatly due to the very different mix proportion from each reference, whether it is paste, mortar or concrete, the compressive strength shows an overall decreasing trend with the increase of *R*.

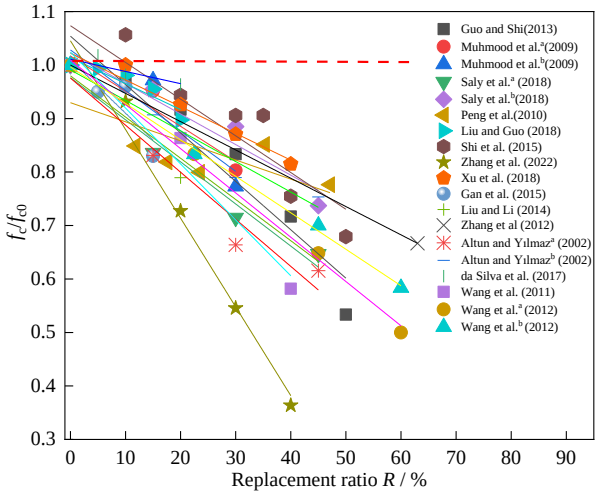


Figure 1. Effect of *R* on f_c/f_{c0} of paste and mortar [26,32–45]. Superscripts letters represents different mix proportion in each reference.

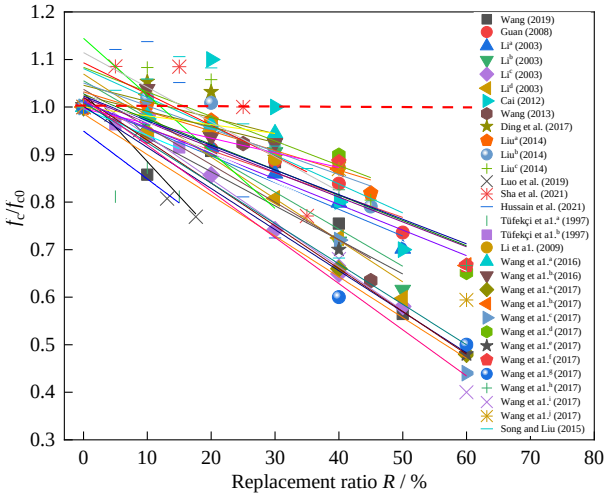


Figure 2. Effect of *R* on f_c/f_{c0} of concrete [23,46–59]. Superscripts letters represents different mix proportion in each reference.

The compressive strength is reduced after the incorporation of SSP. Firstly, compared with cement, SSP contains fewer active substances such as dicalcium silicate (C_2S), tri-

calcium silicate (C_3S), aluminate and ferrialuminate [60–65], the hydration process of the active substances are described by Equations (1)–(4).

$$C_3S + nH_2O \rightarrow C - S - H + (3 - x)Ca(OH)_2 \quad (1)$$

$$C_2S + mH_2O \rightarrow C - S - H + (2 - x)Ca(OH)_2 \quad (2)$$

$$C_3A + 6H \rightarrow C - A - H \quad (3)$$

$$C - A - H + 3C\bar{S}H + 14H \rightarrow +C_3A{\cdot}C\bar{S}{\cdot}H_{32} + CH \quad (4)$$

Here, C = CaO, S = SiO_2, H = H_2O, A = Al_2O_3, $\bar{S} = SO_4^{2-}$.

Secondly, the temperature during the formation of steel slag is relatively high. After the cooling process, the active substance of steel slag forms glass and is wrapped, the vitreous crystal is intact and the grain is large field bond [58]. Under normal circumstances, it is difficult to hydrate. Two factors lead to the reduction of the strength of the cementitious material.

In addition to the above chemical explanations, the surface morphology of SSP particles is closely related to the strength. Due to the difficulty of grinding SSP compared to cement clinker, after grinding, the particles are mostly in the form of flakes, which affects fluidity and is unfavorable for forming a denser slurry structure, resulting in a decrease in strength. However, it should be pointed out that when the grinding process is improved, the roundness of the surface of the SSP is improved, which compensates for fluidity. Some SSP particles also exhibit sponge-like undulations on the surface, which is also beneficial for improving the adhesion between the clinker hydration products and the micro interface of the SSP particles. Therefore, when the hydration performance of cement clinker is poor, it is easy to understand the phenomenon of some strength exceeding the reference strength (R = 0) within the replacement rate of 30% in Figures 1 and 2.

From the key conclusions (Table 2), for most refs., when $R \leq 30\%$, the compressive strength decreases slightly, while once $R > 30\%$, the rate of strength reduction is relatively large. The main reasons are as follows: Due to different proportions, it is possible to use relatively large amounts of cement, resulting in a large number of unhydrated cement particles. At this time, replacing cement with a small amount of SSP ($R \leq 30\%$) will not affect its overall hydration degree. However, when the replacement amount increases ($R > 30\%$), on one hand, the active material will sharply decrease, and the degree of hydration will decrease. On the other hand, the cement hydration reaction will slow down, unable to provide a high alkaline environment, which seriously affects the hydration of SSP and ultimately leads to a significant decrease in strength.

It should be noted that although most of the compressive strength ($R > 0\%$) are smaller than that of control group (R = 0), some references still present special cases, i.e., the strength of certain R are greater than that of the control group. However, the compressive strength improvement rate is not significant, with a maximum of only 14%, and all $R \leq 15\%$ in this scenario.

In addition to the cement strength grade of 52.5R used in ref. [51], in the other references, the cement strength grade is all 42.5, i.e., the research on the replacement of cement with SSP is still focused on the 42.5 grade, and the higher-grade cement is almost not involved. Liu uses early strength cement which is 42.5 R grade [26]. This cement type contributes greatly to the early strength; therefore, the effect of SSP on the early strength should be more obvious. However, the strength data collected in Figures 1 and 2 are all 28-day standard curing, and this effect on early strength is not present in the data.

The ratio of the strength at 90 days $f_{c(90)}$ to 28 days $f_{c(28)}$ is provided to analyze the contribution of SSP to later strength. Figure 3 shows that the $f_{c(90)}/f_{c(28)}$ of all the refs. increase with the increase of R except that of Saly et al. [b] [34]. It indicates that the larger

the R is (the larger the proportion of SSP compares to cement), the better the improvement of the later strength is, i.e., the contribution of SSP to $f_{c(90)}$ is greater than that to $f_{c(28)}$. This is precisely due to the continuous hydration of cement and the increasing alkaline environment, which destroys the amorphous shell of early hydration of SSP, causing the active substances in the SSP to come into contact with water and further hydration reactions.

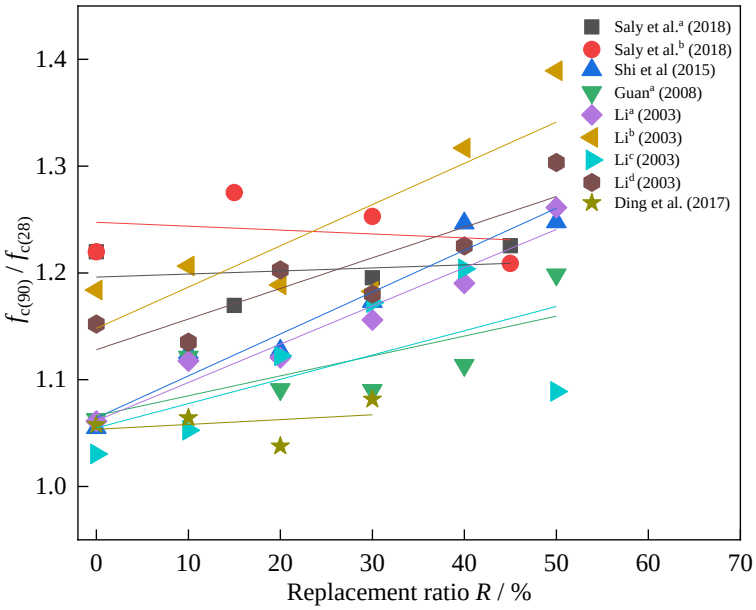


Figure 3. Effect of R on $f_{c(90)}/f_{c(28)}$ [34,37,47,48,51]. Superscripts letters represents different mix proportion in each reference.

Due to the low activity of SSP itself, without chemical improvement and mechanical improvement, the overall strength can only be improved by improving the synergy between Portland cement and its work. When selecting cement, firstly, it is best to choose cement with a fast early hydration reaction. This can quickly improve the environmental alkalinity and stimulate the activity effect of SSP, and due to the slow hydration reaction of SSP, choosing cement with a faster hydration rate also compensates for the insufficient contribution of SSP–cement composite cementitious materials to early strength. Secondly, SSP itself struggles to provide enough active substance; to meet the strength requirements, it is necessary to mix with cement with higher strength. To summarize the above two situations, it is worth considering the self effect of steel slag powder in order to improve the strength of composite materials. Cement with high content of C_3S, C_3A and C_4AF should be selected. Considering the final cementitious effect, cement with a high content of C_3S should be selected. It should be pointed out that there is almost no use of slag cement and fly ash cement in the current research, which is not because the secondary hydration is unfavorable for SSP, but rather that researchers aim to better study the synergistic effect of SSP and pure clinker. The following section will discuss the contribution of adding some mineral admixtures, such as slag and fly ash, to the strength of a ternary cementitious system.

3.2. Replacing Cement with the Mixture of SSP and Slag/Fly Ash

Slag and fly ash are traditional concrete admixtures and a common substitute for cement. Slag is a silicate material similar to cement, with higher hydration ability than SSP [66,67]. The active substance Al_2O_3 and SiO_2 of slag can generate more hydrated calcium silicate (C-S-H) and hydrated calcium aluminate (C-A-H) with the hydration product $Ca(OH)_2$ of SSP, which is called the pozzolanic effect [68]. Its hydration process of the active substances are described by Equations (5) and (6). The presence of f-CaO, f-MgO and RO phases in SSP leads to volume stability issues in concrete [68]. By adding fly ash, the content of f-CaO can be reduced [69].

Combined with the characteristics of slag and fly ash, the SSP–slag or SSP–fly ash are mixed to replace cement in a certain ratio, here referred to as R_c, and the ratio of SSP in the mixture (SSP–slag or SSP–fly) is here referred to as R_s. In total, 16 references and 32 groups are summarized and analyzed. Tables 3 and 4 show the summary for cement replaced with SSP–slag and SSP–fly ash, respectively. All the references (groups) in Tables 3 and 4 conducted three reproducibility tests

$$m\mathrm{Ca(OH)_2} + \mathrm{SiO_2} + \mathrm{H_2O} \rightarrow m\mathrm{CaO{\cdot}SiO_2{\cdot}H_2O} \quad (5)$$

$$m\mathrm{Ca(OH)_2} + \mathrm{Al_2O_3} + \mathrm{H_2O} \rightarrow m\mathrm{CaO{\cdot}Al_2O_3{\cdot}H_2O} \quad (6)$$

Table 3. Summary for cement replacement with SSP–slag.

Reference	R_c (%)	R_s (%)	Strength (Mpa)	Type	Key Conclusions of Different R_c and R_s
Guo and Shi [b] [32]	0~100	0, 50	60, 58~33	paste	The strength decreases with the increase of R_s.
Muhmood et al. [c] [33]	0, 40	0, 50	66.5, 58.6~58	paste	The strength decreases by adding SSP and slag.
Muhmood et al. [d] [33]	0, 40	0, 50	66.5, 58.6~61		
Gan et al. [b] [40]	0~40	0, 50	53, 64~57	mortar	The strength decreases with the increase of R_s and the slag improves it.
Zhang et al. [b] [41]	0, 100	0, 63	51, 41, 34	mortar	SSP reduces the strength more compare slag.
Wang et al. [c] [45]	30, 50	0, 50	46, 45, 42	concrete	The strength decreases with the increase of R_s from 30% to 50%.
Guan [b] [47]	0~50	50	65.1~43.9	concrete	The strength decreases with the increase of R_c when R_s = 50%.
Li [e] [48]	0~50	50	67.1~44.8	concrete	The strength decreases with the increase of R_c when R_s = 50%.
Li [f] [48]	0~50	50	48.4~31.2		
Li et a1 [b] [56]	0~67	0, 30	55, 53~45	concrete	The strength decreases with the increase of R_s.
Liao [70]	0~50	40	40.2~42.6~39	concrete	With the increase of R_c, the strength first increases and then decreases, and the highest strength is 42.6 MPa when R_c = 40%.
Shi [a] [71]	0~100	30	67~52	concrete	Compared with SSP, slag contributes more to the strength. The strength decreases with the increase of R_s.
Yang [a] [72]	0~40	40	56~52	concrete	At high water–cement ratio, the strength decreases with the increase of R_s, which increases at a low–water cement ratio.
Yang [b] [72]	0~40	30	77~82	concrete	The strength increases with the increase of R_s at a low water–cement ratio, and has a mutual effect with slag.
Song [a] [73]	0~100	30	44.0~35.1	paste	The strength decreases with the increase of R_s, and the strength is the highest when the R_s = 20%~30%.
Wang [74]	20~80	0, 50	64, 62.8~39.4	concrete	The strength decreases with the increase of R_s.
Liu [75]	0~50	50	55~33.5	concrete	The strength decreases with the increase of R_s. The slag contributed more to the strength.
Li [76]	0~100	0, 30	56,46~54~45	concrete	The strength first increases and then decreases with the increase of R_s. The highest compressive strength is 54MPa, when R_s = 67%.

Note: Superscripts a–f represents different mix proportion in each reference.

It can be seen from Figures 4 and 5 that only the strength of Yang [b] [72], Muhmood et al. [d] [33] and Cai [b] [49] show increasing trends, the strength of most groups decrease with the increase of R_c when R_c = 0%~100%. However, the decreasing trends are not obvious compared to Figures 1 and 2. This indicates that replacing cement with the mixture of SSP and slag/fly ash are relatively better than using only SSP. Figures 6 and 7 show that when R_c = 50%, the strength of all the groups decrease significantly with the increase of R_s. This is the same conclusion as the increase of R in the previous section, i.e., the contribution of SSP to strength is less than slag and fly ash. However, Liao [70] shows that when R_s = 40%, the strength does not change significantly with the increase of R_c, which means that the effect of strength reduction after the increase of R_c is offset when the amount of slag is higher than that of SSP.

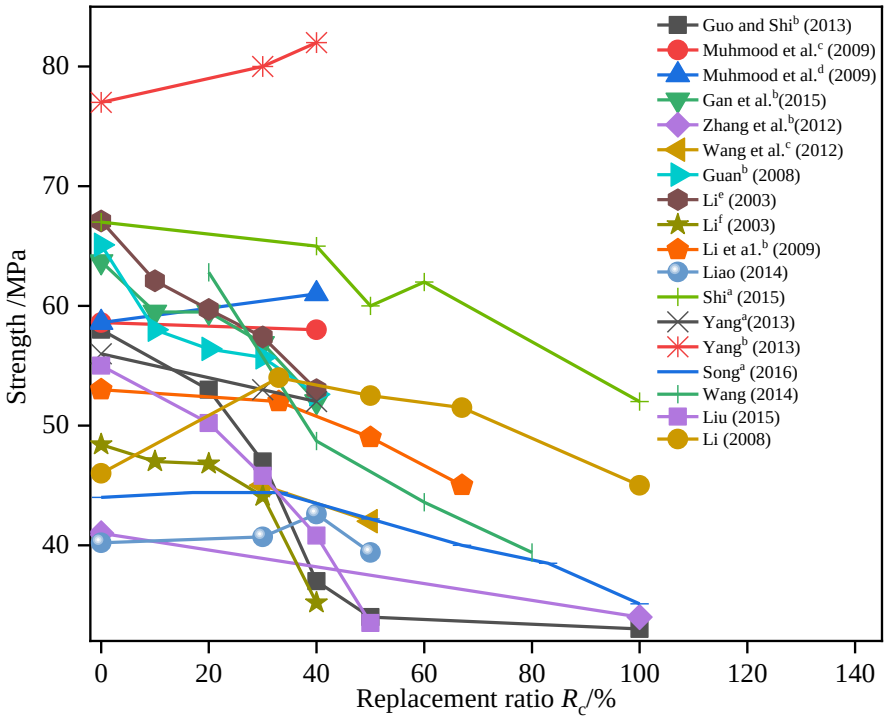


Figure 4. Effect of R_c on strength of cement-based composite with SSP and slag [32,33,40,41,45,47,48,56,70–76]. Superscripts letters represents different mix proportion in each reference.

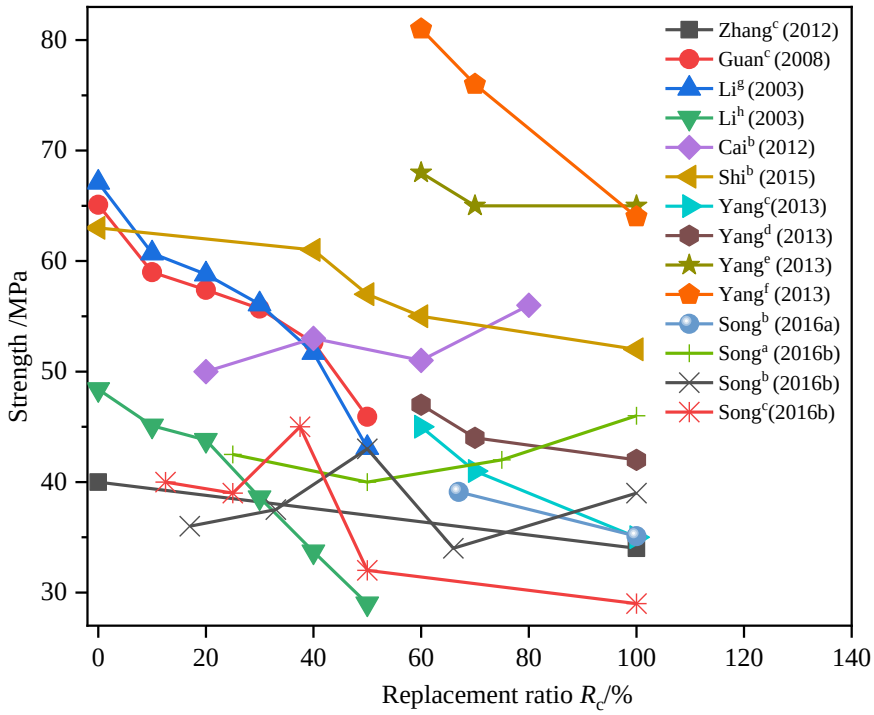


Figure 5. Effect of R_c on strength of cement-based composite with SSP and fly ash [41,47–49,71–73,77]. Superscripts letters represents different mix proportion in each reference.

Table 4. Summary for cement replacement with SSP- fly ash.

Reference	R_c (%)	R_s (%)	Strength (Mpa)	Type	Key Conclusions of Different R_c and R_s
Zhang [c] [41]	0, 100	0, 63	51, 40, 34	mortar	The strength decreases with the increase of R_s.
Guan [c] [47]	50	0~50	65.1~45.9	concrete	The strength decreases with the increase of R_c. When $R_c \geq 40\%$, it decreases quickly.
Li [g] [48]	50	0~50	67.1~43.1	concrete	The strength decreases with the increase of R_c and that of low water cement ratio decreases more obviously.
Li [h] [48]	50	0~50	48.4~29.0		
Cai [b] [49]	20~80	50	50~56	concrete	The strength slightly increases with the increase of R_s.
Shi [b] [71]	0~100	30	62.5~52	concrete	The strength decreases with the increase of R_s. When the $R_s \geq 40\%$, it decreases quickly.
Yang [c] [72]	60~100	0, 35	50, 45~35	concrete	The strength decreases with the increase of R_c and R_s. The strength of low water cement ratio is significantly higher than that of high water cement ratio.
Yang [d] [72]	60~100	0, 20	50, 47~42		
Yang [e] [72]	60~100	35	75, 68~54		
Yang [f] [72]	60~100	20	75, 81~64		
Song [b] [73]	67~100	30	39.1~35.1	paste	The strength decreases with the increase of R_s.
Song [a] [77]	25~100	20	42.5~46	concrete	R_s has a greater impact on compressive strength with the increase of R_c.
Song [b] [77]	17~100	30	36~43~39		
Song [c] [77]	13~100	40	40~45~29		

Note: Superscripts a–h represents different mix proportion in each reference.

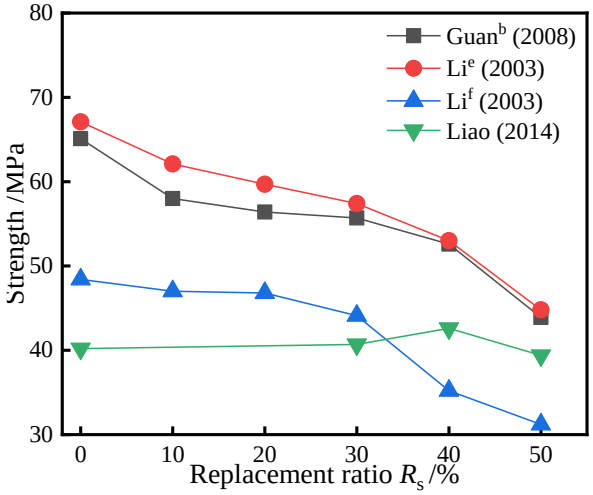


Figure 6. Effect of R_s on strength with SSP and slag [47,48,70]. Superscripts letters represents different mix proportion in each reference.

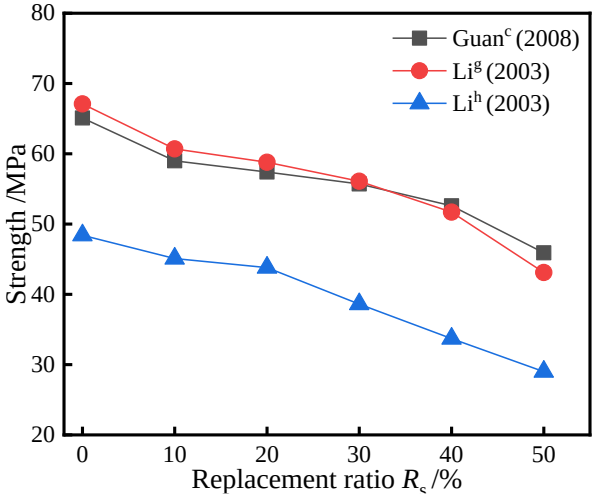


Figure 7. Effect of R_s on strength with SSP and fly ash [47,48]. Superscripts letters represents different mix proportion in each reference.

The effect of replacing cement with SSP, slag and fly ash on strength of concrete have also been studied. Because the activity of fly ash is lower than that of slag, and the early hydration rate is slow, the early strength is not high when fly ash and SSP are

mixed as admixtures. However, this does not affect the development of concrete in the later period [78–80]. When the $R_c \leq 40\%$, the strength of the cement-based composite is improved when the ratios of SSP, slag and fly ash are 1:2:1 [59]. This indicates that the selection of appropriate ratios can ensure the strength of concrete, which is not only in accordance with the concept of green development, but also can reduce the cost of concrete production.

3.3. Effect of Specific Surface Area (SSA) on Strength

SSA is an important physical characteristic of cementitious materials. Cement, as the current main cementitious material, has a significant impact on the hydration reaction due to having a different SSA [81]. The degree of hydration reaction will also directly affect the strength of the material. In addition, some admixtures, such as slag and fly ash, have also conducted relevant studies on the Effect of SSA on strength [82]. Therefore, the impact of changes in the SSA of SSP on strength cannot be ignored. A total of six references and nine groups are summarized and analyzed. The summary of different SSA of SSP for cement-based composite is shown in Table 5 and all the references (groups) conducted three reproducibility tests.

Table 5. Summary of different SSA of SSP for cement-based composite.

Reference	*R* (%)	SSA (m^2/kg)	Strength (Mpa)	Type	Key Conclusions of Strength–SSA
Liu and Li [26]	45	398~635	37~44	concrete	The strength increases with the increase of SSA.
Li [i] [48]	30	400~800	52.5~59.5~58	concrete	The strength increases first and then decreases with the increase of SSA.
Liao [70]	25	390~646	43.2~50.8	concrete	The strength increases with the increase of SSA.
Yang et al. [a] [83]	10	350~550	54.1~58.6	concrete	The strength increases with the increase of SSA and decreases with the increase of *R*.
Yang et al. [b] [83]	20	350~550	48.7~57.1		
Yang et al. [c] [83]	30	350~550	43.5~49.4		
Yang et al. [d] [83]	40	350~550	37.4~47.2		
Ma [84]	17.6	480~720	46.8~54	concrete	The strength increases with the increase of SSA.
Liu [85]	30	615~683	29~30.5	concrete	The strength increases slightly with the increase of SSA.

Note: Superscripts a–d and i represents different mix proportion in each reference.

Figure 8 shows that increasing the SSA of SSP can significantly improve the strength of concrete. First, it increases the contact area of SSP and water, so that C_2S and C_3S in SSP can quickly and fully conduct a hydration reaction, and generate more C-S-H [86]; second, the mechanical force to recrystallize the lattice of SSP vitreous, form a noncrystallographic state that readily reacts with water, which accelerates the hydration reaction, and then, form the alkaline environment to stimulate the SSP [87]. Third, due to the high SSA, the remaining SSP without hydration exerts the microaggregate effect of filling. By reducing cracks and enhancing the compactness to improve the strength of concrete.

The strength growth rate can be divided into two parts of each reference which can be seen from Figure 8 by using vertical solid lines. For most refs., the strength growth rate of the first part is large, and the second part is small. The ranges of two parts and the strength growth rate of them are shown in Table 6.

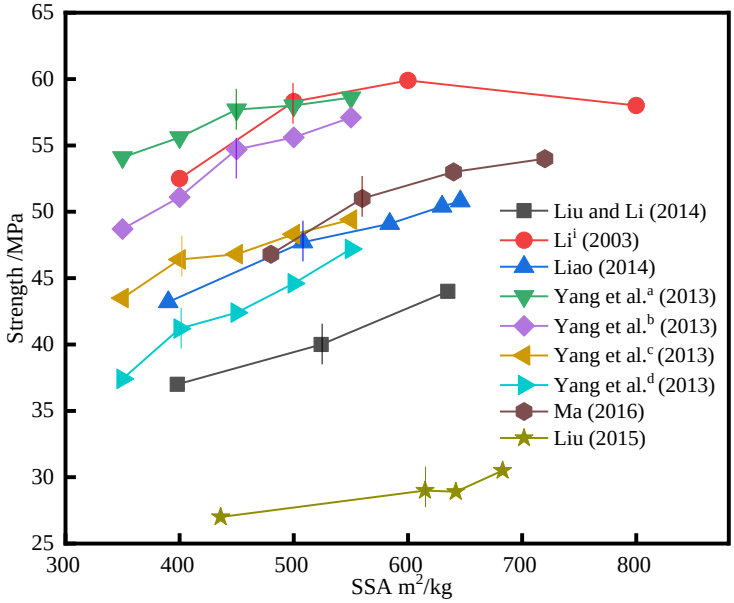


Figure 8. Effect of SSA of SSP on compressive strength [26,48,70,83–85]. Superscripts letters represents different mix proportion in each reference.

Table 6. Ranges of two parts and the strength growth rate.

References	1st Part (m^2/kg)	Strength Growth Rate of 1st Part %	2nd Part (m^2/kg)	Strength Growth Rate of 2nd Part %
Liu and Li [26]	398~524	2.4	524~635	3.6
Li [i] [48]	400~500	5.8	500~600	1.6
Liao [70]	390~508	3.0	508~646	2.2
Yang et al. [a] [83]	350~450	3.6	450~550	0.9
Yang et al. [b] [83]	350~450	6.0	450~550	2.4
Yang et al. [c] [83]	350~400	5.8	400~550	2.0
Yang et al. [d] [83]	350~400	7.6	400~550	4.0
Ma [84]	480~560	5.3	560~720	1.9
Liu [85]	436~615	1.1	615~683	2.2

Note: Superscripts a–d and i represents different mix proportion in each reference.

Table 6 shows that the strength growth rates of the first part of all refs. are between 1.1% and 7.6%, with an average of 4.4%. Those of the second part are between 0.9% and 3.6%, with an average of 2.3%. The vertical solid lines of all refs. are mainly between 400 m^2/kg and 500 m^2/kg in SSA axis. Therefore, further increasing the SSA to improve the strength is not the best method when the SSA is larger than 500 m^2/kg. Considering the income ratio, the SSA should be between 400 m^2/kg and 500 m^2/kg.

It is noted that the strength growth rates of the two parts are both the largest in Yang et al. [d] [83], compare Yang et al. [a] [83], Yang et al. [b] [83] and Yang et al. [c] [83]. The R = 40% of Yang et al. [d] [83] is also the largest compared to the other three groups (R = 10%, 20%, 30%) from Table 5. This indicates that the greater the R, the greater the contribution of SSA to strength.

It should be pointed out that when the SSA is in the range of (600~800) in Li [i] [48], its strength growth rate is −1.0%. This is mainly due to the large interaction between the SSP particles. When the SSA is too large, the active components in SSP agglomerate, reduces the contact surface between SSP and water, and reduces the hydration reaction rate and final strength [88–90]. It is not advisable to increase the SSA to obtain higher strength.

3.4. Effect of Chemical Activated SSP on Strength

Using chemical activators to activate SSP is another important method to improve the strength. In recent years, research on the types and dosages of chemical activators has been carried out [64,88–94]. Details of common chemical activators are shown in Table 7. Due to the unfavorable corrosion resistance of acidic activators on reinforced concrete structures, the vast majority of research on activators revolves around two types of activators: salt and alkali. In general, the most commonly used salt and alkaline activators are sodium and potassium-based solutions, including silicates, hydroxide, sulfate and carbonate. A total of 5 references and 17 groups of data are summarized and analyzed. Table 8 shows the different activators that activate SSP for cement-based composite. All the references (groups) conducted three reproducibility tests.

Table 7. Types of chemical activators.

Activated Types	Activators	Characteristic(s)
alkali activators	NaOH, $Ca(OH)_2$, etc.	By directly providing an alkaline environment, the vitreous hydration of SSP is activated.
salt activators	Na_2SO_4, Na_2CO_3, $NaAlO_2$, Na_2SiO_3, etc.	The provided negative ions can combine with the positive ions contained in SSP to generate the substance contributing to the cementitious material.
acidic activators	H_2SO_4, H_2CO_3, etc.	By providing acidic environment, the glass body depolymerization of SSP is promoted and the hydration reaction is improved.

Table 8. Summary of different activators activate SSP for cement-based composite.

Reference	Activators	Dosages (%)	*R* (%)	Strength (MPa)	Key Conclusions of Strength Dosages with Different Activators
Zhang et al. [a] [38]	Na_2SiO_3	0, 4	10	41.5~44	The strength increases with the increase of dosages, except *R* = 40%
Zhang et al. [b] [38]	Na_2SiO_3	0, 4	20	32~39	
Zhang et al. [c] [38]	Na_2SiO_3	0, 4	30	24~30	
Zhang et al. [d] [38]	Na_2SiO_3	0, 4	40	26~25	
Zhang et al. [41]	Na_2SiO_3 + CaO+ $KAl(SO_4)_2$	0, 3	32	42~48	The strength increased from 42 MPa to 48 MPa with the addition of composite activator.
Wang [a] [95]	Na_2SO_4	0~2.5	100	32.3~43~33.1	The strength increases first and then decreases with the increase of Na_2SO_4.
Wang [b] [95]	Na_2SiO_3	0~2.5	100	32.3~46.3~42.6	The strength increases first and then decreases with the increase of Na_2SiO_3
Wang [c] [95]	$NaAlO_2$,	0~2.5	100	32.3~46.7	The strength increases with the increase of $NaAlO_2$.
Wang [d] [95]	Na_2SO_4 + $NaAlO_2$	0, 2	100	32.3~44.2	The strength increases with the increase of Na_2SO_4 + $NaAlO_2$.
Wang [e] [95]	Na_2SO_4 + Na_2SiO_3	0, 2	100	32.3~42.5	The strength increases with the increase of Na_2SO_4 + Na_2SiO_3.
Dong [a] [96]	Na_2SO_4	0~4	100	33.4~42.2~38.9	The strength is the highest at a dosage of 2% with Na_2SO_4
Dong [b] [96]	Ca_2SO_4	0~4	100	33.5~42.3~40.9	The strength is the highest at a dosage of 3% with Ca_2SO_4
Dong [c] [96]	NaOH	0~2	100	33.5~39.4~35.7	The strength is the highest at a dosage of 1.5% with NaOH.
Dong [d] [96]	$Ca(OH)_2$	0~2	100	33.5~42~41.1	The strength is the highest at a dosage of 1% with Ca $(OH)_2$
Dong [e] [96]	Na_2SiO_3	0~4	100	33.5~38.2~35.6	The strength is the highest at a dosage of 2% with Na_2SiO_3.
Dong [f] [96]	$NaAlO_2$	0~4	100	33.5~43.7~40.2	The strength is the highest at a dosage of 3% with $NaAlO_2$.
Sun [14]	Na_2SiO_3	0.5~2	100	10~14	With the increase of Na_2SiO_3, the strength increases.

Note: Superscripts a–f represents different mix proportion in each reference.

Figure 9 shows that after chemical activation of SSP, the strength is significantly affected. With the increase of the dosages of the activator, the strength first increases and then decreases for most refs. The optimal dosages of activator are between 1.0% and 3.0%. It should be pointed out that in Sun [14], 100% SSP is used, i.e., *R* = 100%. Therefore, its strength is significantly lower than other refs. Meanwhile, due to the lack of cement, the

alkaline environment is severely insufficient, resulting in a significant improvement in the alkaline environment and an increase in strength after an increase in Na_2SiO_3 between 0.5% and 2%. In addition, in Zhang et al. [a] [38], there is only one dosage variable, so only linear results are given, and it is not possible to characterize whether there is a nonlinear change in strength of the dosage between 0 and 4%, and whether there is a threshold between them still needs further verification.

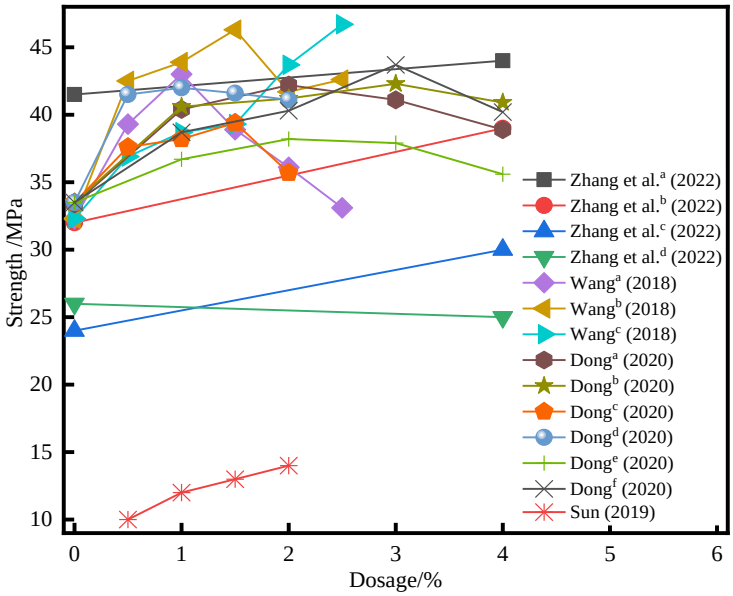


Figure 9. Effect of different dosage of one activator on strength [14,38,95,96]. Superscripts letters represents different mix proportion in each reference.

The alkaline environment produced by alkali activator causes the SSP glass body to form high-strength zeolite products through two processes of decomposition and polymerization. It is found that the main structural forming bonds of SSP glass body are Si-O and Al-O bond, which exist in the form of $[SiO_4]$ and $[AlO_4]$ tetrahedron or $[AlO_4]$ coordination polyhedron, respectively [97]. The OH-ions provided by alkali activator can make $[SiO_4]$ tetrahedron decompose to form $H_3SiO_4^-$, $[AlO_4]$ tetrahedron decompose to form $H_3AlO_4^{2-}$, $[AlO_6]$ coordination polytopes decomposition into $Al(OH)^{2+}$, then $H_3SiO_4^-$ and $H_3AlO_4^{2-}$ polymerization with Ca^{2+} and Na^+ to generate zeolite hydration product [98],(Equations (3) and (4)). $Al(OH)^{2+}$, $H_3SiO_4^-$, OH^-, Ca^{2+} and Na^+ also converge to produce zeolite hydration products, as shown in Equations (7) and (10).

$$H_3SiO_4^- + H_3AlO_4^{2-} + Ca^{2+} \rightarrow kCaO{\cdot}jAlO_2{\cdot}mSiO_2{\cdot}nH_2O \quad (7)$$

$$H_3SiO_4^- + H_3AlO_4^{2-} + Ca^{2+} + Na^+ \rightarrow pNaO{\cdot}kCaO{\cdot}jAlO_2{\cdot}mSiO_2{\cdot}nH_2O \quad (8)$$

$$Al(OH)^{2+} + H_3SiO_4^- + OH^- + Ca^{2+} \rightarrow kCaO{\cdot}jAlO_2{\cdot}mSiO_2{\cdot}nH_2O \quad (9)$$

$$Al(OH)^{2+} + H_3SiO_4^- + OH^- + Ca^{2+} + Na^+ \rightarrow pNaO{\cdot}kCaO{\cdot}jAlO_2{\cdot}mSiO_2{\cdot}nH_2O \quad (10)$$

Due to the stable zeolite hydration products generated by the reaction of $[AlO_4]$ tetrahedral and $[AlO_6]$ coordination polyhedral, the $H_3SiO_4^-$ decomposed by $[SiO_4]$ tetrahedral is consumed, promoting the reaction to proceed continuously, and the forming bonds Si-O and Al-O of the steel slag vitreous are constantly destroyed. The hydration products of zeolite generated by the glass body depolymerization have high strength and durability, and they are constantly interwoven and connected, making the cementitious structure

gradually formed and strengthened [97]. It is found that sodium silicate only acts as a skeleton network in SSP, and as a hydration gel it plays a mosaicism and filling role in the network, while Na^+ in sodium silicate mainly maintains the PH value of the solution and plays a catalytic role in the dissociation of SSP vitreous, and it does not participate in the reaction formation of hydration products [99]. When SSP and cement are used as cementitious materials, $Ca(OH)_2$ generated by cement hydration can also provide an alkaline environment for SSP, but the excitation magnitude is small, so the amount of activators depends on the alkalinity of the environment during hydration. On the premise of ensuring the excitation of SSP, the cost caused by the amount of activators should be reduced. SO_4^{2-} ion from sulfate decomposition reacts with Ca^{2+} ion from cement hydration and active Al_2O_3 from SSP to generate ettringite (AFt) (Equation (11)). It not only has high strength but also has a certain expansion effect, which can fill the pores in the hydration space and improve the compactness of cement paste. At the same time, SO_4^{2-} replaces the SiO_4^{2-} ion in calcium silicate hydrate, which can promote the hydration reaction of steel slag to generate C-S-H gel and C-A-H crystals [100].

$$Al_2O_3 + 6Ca^{2+} + 3SO_4^{2-} + 6OH^- + 29H_2O \rightarrow 3CaO{\cdot}Al_2O_3{\cdot}CaSO_4{\cdot}32H_2O\ (AFt) \quad (11)$$

Figure 10 shows that the effect of mix activators on strength improvement is more significant when the dosage is within 3%. After excitation with mix activators, the diffraction peaks of calcium hydroxide, calcium silicate and calcium silicate are low compared to excitation with one activator. This shows that more tricalcium silicate and dicalcium silicate in the SSP undergo hydration reactions. It can be seen that the amount of the needle, rod Aft crystal and amorphous C-S-H increased significantly. However, the dosage generally does not exceed 2%, and if the OH^- content is too high it will prevent the process of hydration of cement material to produce calcium hydroxide and the fluidity of SSP and cement will be reduced. Due to the high alkali content, it may cause engineering problems such as alkali aggregate reaction and alkali spreading.

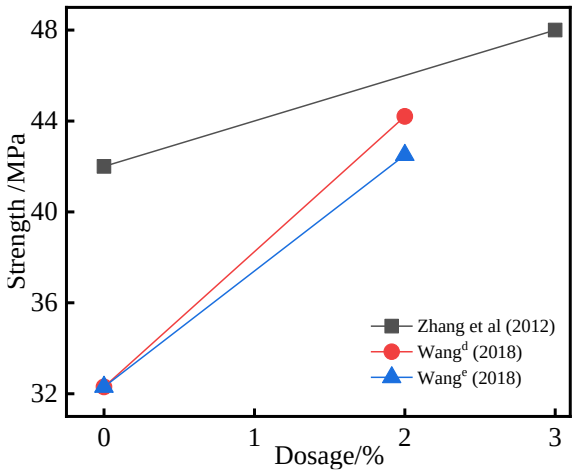


Figure 10. Effect of different dosage of mix activators on strength [41,95]. Superscripts letters represents different mix proportion in each reference.

In addition, the research results also show that Na_2SO_4 and NaOH are beneficial to the early strength development, and Ca_2SO_4 and $Ca(OH)_2$ are beneficial to the later strength development. Wu shows that when using silica fume or Na_2SiO_3 as activators, the strength in both the early and late stages are better [101].

3.5. Effect of Different Curing and Age t on Strength

Curing conditions are divided into natural curing (with a room temperature of 20 ± 2 °C and a relative humidity of 50%), standard curing (with a standard curing temperature of

20 ± 2 °C and a relative humidity of 98%), steam curing, hot and heat curing, high-temperature curing and hot water curing at present. The high-temperature curing mode also becomes thermodynamic excitation. A total of 5 references and 12 groups of data under different curing are summarized and analyzed. The curing and *R* of each reference are shown in Table 9. The effects on the strength with the increase of age *t* are shown in Figure 11, in which each point is the average value of three reproducibility tests.

Table 9. Curing conditions and mix proportion.

Reference	Curing Condition	*R* (%)
Cui et al. [102]	Standard curing, hot and heat curing (56 °C and 90 °C)	20
Liu et al. [103]	Standard curing, steam curing (100 °C)	5
Zhang et al. [104]	Natural curing, standard curing	20
Zhang et al. [105]	Natural curing, standard curing, hot and heat curing (50 °C)	5
Wang [106]	Natural curing, standard curing	7.5

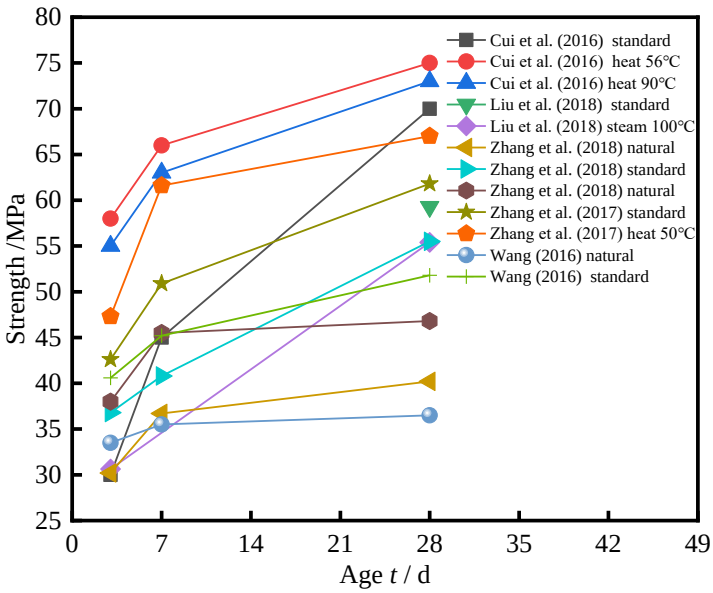


Figure 11. Effect of age *t* on compressive strength of SSP under different curing methods [102–106].

Figure 11 shows that with the increase of *t*, the compressive strength increase, and the rate of compressive improvement from 3 d~7 d is large, while from 7 d~28 d turn to small. The hot- and heat-curing methods have a more obvious effect on the compressive strength growth of SSP gel material, i.e., the more significant the compressive strength in the early stage, the later strength is almost the same. Cui et al. [102] show that excessive temperature will lead to dehydration and recrystallization of calurite, the hydration product of SSP, which is adverse to the late stability of concrete; Zhang et al. [105] show that the effect of the curing methods on the compressive strength is as follows: hot and heat curing > standard curing > natural curing. It should be pointed out that Liu et al. [103] show that the compressive strength under standard curing is 59.29 MPa at 28 d, which is larger than 55.39 MPa under steam curing. Although the steam curing is conducive to the early strength development, the hydration product is not homogeneous enough, and the standard conservation has an adequate water supply, which can make the cementitious material hydration more sufficient.

Based on the above analysis the following can be concluded: firstly, under natural curing, the temperature and humidity of concrete cannot be met under dry and normal temperature conditions. As the hydration reaction progresses, combined with the consumption of mixing water and partial evaporation into the air with pores, incomplete hydration and an increase in concrete voids are caused. However, standard curing has appropriate temperature and humidity, which is conducive to the normal hydration of concrete. Secondly, the steam curing can not only improve the hydration rate of clinker, but also accelerate the secondary hydration reaction rate of mineral admixtures. The early hydration products of SSP have certain strengths. Thirdly, hot and heat curing has a positive effect on the hydration of SSP, especially in accelerating the early hydration rate and generating more hydration products. In addition, some of the literature suggests that under the action of high temperature and pressure, the main structural bonds forming the Si-O and Al-O bonds of the steel slag glass body will be interrupted, increasing the hydration rate of the steel slag.

3.6. Effect of Different R on Heat of Hydration

The hydration heat is the heat released when a cementitious material combines with water. Generally speaking, the greater the hydration heat, the more cementitious products and the higher the strength is. Therefore, the strength of cement-based composites can be indirectly measured by the hydration heat.

At present, the hydration heat is mainly measured using the national standard "Cement Hydration Heat Test Method (Direct Method)" GB2022-80, with a temperature controlled at around 25 °C. The content includes the hydration heat evolution rate and cumulative hydration heat. The measurement time of hydration heat is generally within 7 days, and the typical record time points are the first day, third day and seventh day. A summary of some research on the hydration heat of the mixture of SSP and cement is shown in Table 10.

Table 10. Summary of the hydration heat of the mixture of SSP and cement.

Reference	*R* (%)	Type	Hydration Heat			Description/Unit
			1st d	3rd d	7th d	
Liu and Li [26]	0, 20, 45	paste	– – –	– – –	282.0, 224.9, 162.1 282.0, 230.1, 164.2 282.0, 236.0, 162.7	Cumulative/(J/g)
Wang et al. [a] [45]	0, 20 0, 40 0, 60	paste	5.3, 5.2 5.3, 4.0 5.3, 2.4	2.2, 1.5 2.2, 1.2 2.2, 1.0	– – –	Rate/ J/(gh)
Guan [a] [47]	0, 30	paste	187.6, 117.6	240.0, 169.8	271.3, 206.1	Cumulative/(J/g)
Li [a] [48]	0, 40	paste	176.3, 112.0	228.0, 159.9	255.0, 193.4	Cumulative/(J/g)
Song [a] [73]	0, 30	paste	77.3, 54.1	113.0, 79.1	133.4, 93.4	Cumulative/(J/g)
Han et al. [107]	0~50	paste	220~100	275~140	290~150	Cumulative/(J/g)
Zhuang and Wang [108]	0, 30	paste	210, 75	260, 150	290, 205	Cumulative/(J/g)
Sun et al. [15]	0, 100	mortar	210, 95	260, 120	280, 130	Cumulative/(J/g)
Zhang et al. [42]	0, 63	paste	180,50	199,75	205,85	Cumulative/(J/g)

Note: Superscripts a represents different mix proportion in each reference.

From Table 10, it can be seen that at the first day, third day and seventh day, with the increase of *R*, the cumulative hydration heat significantly decreases, which is significantly different from the hydration heat of pure cement. The hydration heat evolution rate decreases with the increase of *R* and also with the increase of age.

The above conclusion indicates that, while meeting the strength requirements, the addition of SSP can significantly reduce the stress inside on large-volume concrete. SSP can be used as a cementitious material to reduce the adverse effects of a high hydration zone.

4. Conclusions

The large-scale use of SSP as a cementitious material instead of cement is beneficial for both the economy and the environment. This paper summarizes and analyzes the effects of SSP on the compressive strength of cement-based composites from multiple aspects, and obtains the following conclusions:

(1) When using SSP to replace cement as a cementitious material, the strength shows an overall decreasing trend with the increase of R. In terms of mineral composition, compared to cement, the active substances in SSP are relatively less, which limits the hydration reaction and leads to insufficient cementitious composition, resulting in a decrease in strength. In terms of physical properties, Due to the particles of SSP are mostly in the form of flakes, which affects fluidity and is unfavorable for forming a denser slurry structure, resulting in a decrease in strength.

(2) When using a mixture of SSP and slag/fly ash instead of cement, the strength of most groups decreases with the increase of R_s, but the downward trend is not significant; This is due to the secondary hydration reaction between silica and alumina in slag and fly ash and calcium hydroxide to generate hydrated calcium silicate. Compared to slag and fly ash, the contribution of SSP to strength is relatively poor.

(3) When only one activator is used for excitation, the compressive strength usually increases first and then decreases within the 4% range as the dosage of a single activator increases. It indicates that there is an optimal amount of SSP excited using a single activator. Within the range of 3%, the effect of mixing multiple activators is better than that of a single activator.

(4) The compressive strength increases with the increase of SSA. This is because mechanical force crushes the active glass crystals in SSP, increasing the contact area between the active substance and water, and improving the hydration reaction. However, when SSA is too high, it will reduce its strength, which is caused by the aggregation effect of SSP. Considering the preparation cost, the optimal range of SSA is 400 m^2/kg to 500 m^2/kg.

(5) With the increase of age t, the compressive strength of cement-based composite with SSP increases. The increase rate of strength in the first 7 days is significantly greater than that from the 7th to 28th days. The effect of curing methods on compressive strength is in the following order: hot and heat curing > standard curing > natural curing. Due to the possibility of insufficient moisture in steam curing, its effectiveness may be worse than standard curing, and more experiments are needed to verify.

(6) SSP has a significant impact on the hydration heat of composite cementitious systems. With the increase of R, the cumulative hydration heat significantly decreases, which is significantly different from the hydration heat of pure cement. The hydration heat evolution rate decreases with increase of R and also with the increase of age.

Author Contributions: Conceptualization, G.S. and S.J.; formal analysis, C.L.; investigation, G.S.; data curation, C.L.; writing—original draft preparation, G.S.; writing—review and editing, G.S.; visualization, C.L.; supervision, Q.B.; project administration, G.S. All authors have read and agreed to the published version of the manuscript.

Funding: This work was financially supported by the Natural Science Foundation of China (51978417), the Technology Project Funded by Liaoning Provincial Department of Communications (2023034) and Social Governance Science and Technology Special Project Funded by Shenyang in 2020 (20-206-4-11).

Data Availability Statement: Not applicable.

Conflicts of Interest: The authors declare no conflict of interest.

References

1. Faraone, N.; Tonello, G.; Furlani, E.; Maschio, S. Steelmaking Slag as Aggregate for Mortars: Effects of Particle Dimension on Compression Strength. *Chemosphere* **2009**, *77*, 1152–1156. [CrossRef] [PubMed]
2. Furlani, E.; Tonello, G.; Maschio, S. Recycling of Steel Slag and Glass Cullet from Energy Saving Lamps by Fast Firing Production of Ceramics. *Waste Manag.* **2010**, *30*, 1714–1719. [CrossRef] [PubMed]
3. Fang, M.; Fang, G.; Xia, Y.; Wang, H.Y. Study on Compressive Strength of Concrete Mixed by SSP and Fly Ash. In *IOP Conference Series: Earth and Environmental Science*; IOP Publishing: Bristol, UK, 2020; Volume 508, p. 012183.
4. Yi, H.; Xu, G.; Cheng, H.; Wang, J.S.; Wan, Y.F.; Chen, H. An overview of Utilization of Steel Slag. *Procedia Environ. Sci.* **2012**, *16*, 791–801. [CrossRef]
5. Salazar, K. *Mineral Commodity Summaries 2013: US Geological Survey (USGS)*; J. US Geological Survey: Reston, VA, USA, 2013.
6. Summaries, U.M.C.; Series, U.U. *Mineral Commodity Summaries 2019: US Geological Survey (USGS)*; J. US Geological Survey: Reston, VA, USA, 2019.
7. Yang, X.B.; Dong, F.S.; Zhang, X.Z.; Li, C.Z.; Gao, Q. Review on Comprehensive Utilization of Magnesium Slag and Development Prospect of Preparing Backfilling Materials. *Minerals* **2022**, *12*, 1415. [CrossRef]
8. Cheng, X.X.; Yang, Q.B. Comprehensive Utilization of Steel Slag. Chin. *Fly Ash Compr. Util.* **2010**, *5*, 45–49.
9. Motz, H.; Geiseler, J. Products of Steel Slags an Opportunity to Save Natural Resources. *Waste Manag.* **2001**, *3*, 285–293. [CrossRef] [PubMed]
10. Sun, J.; Liu, W.; Hu, Y.; Wu, J.Q.; Li, M.K.; Yang, X.W.; Wang, W.Y.; Xu, M. Enhanced Performance of Extruded-spheronized Carbide Slag Pellets for High Temperature CO_2 Capture. *Chem. Eng. J.* **2016**, *285*, 293–303. [CrossRef]
11. Shi, C.; Qian, J. High Performance Cementing Materials from Industrial Slags—A Review. *Resour. Conserv. Recycl.* **2000**, *29*, 195–207. [CrossRef]
12. Nguyen, T.T.H.; Phan, D.H.; Mai, H.H.; Nguyen, D.L. Investigation on Compressive Characteristics of Steel-slag Concrete. *Materials* **2020**, *13*, 1928. [CrossRef] [PubMed]
13. Mo, L.; Zhang, F.; Deng, M.; Jin, F.; Al-Tabbaa, A.; Wang, A.G. Accelerated Carbonation and Performance of Concrete Made with Steel Slag as Binding Materials and Aggregates. *Cem. Concr. Comp.* **2017**, *83*, 138–145. [CrossRef]
14. Sun, J.; Chen, Z. Effect of Silicate Modulus of Water Glass on the Hydration of Alkali-activated Converter Steel Slag. *J. Therm. Anal. Calorim.* **2019**, *138*, 47–56. [CrossRef]
15. Sun, J.; Zhang, Z.; Zhuang, S.; He, W. Hydration Properties and Microstructure Characteristics of Alkali–activated Steel Slag. *Constr. Build. Mater.* **2020**, *241*, 118141. [CrossRef]
16. Sheng, G.H.; Jin, S.J.; Li, C.; Bai, Q.; Wang, X.Y. Compressive-Tensile Mechanics and Energy Consumptions of a Cementitious Composite with High Utilization of Steel Slag. *KSCE J. Civ. Eng.* **2023**, *27*, 1236–1248. [CrossRef]
17. Khater, A.M.; Soliman, A.; Ahmed, T.S.; Ismail, I.M. Power Generation in White Cement Plants from Waste Heat Recovery Using Steam-organic Combined Rankine cycle. *Case Stud. Chem. Environ. Eng.* **2021**, *4*, 100138. [CrossRef]
18. Sahoo, N.; Kumar, A.; Samsher, S. Review on Energy Conservation and Emission Reduction Approaches for Cement Industry. *Environ. Dev.* **2022**, *44*, 100767. [CrossRef]
19. Wojtacha-Rychter, K.; Kucharski, P.; Smolinski, A. Conventional and Alternative Sources of Thermal Energy in the Production of Cement—An Impact on CO_2 Emission. *Energies* **2021**, *14*, 1539. [CrossRef]
20. Dinga, C.D.; Wen, Z. China's Green Deal: Can China's Cement Industry Achieve Carbon Neutral Emissions by 2060. *Renew. Sust. Energ. Rev.* **2022**, *155*, 111931. [CrossRef]
21. Shi, C. Steel Slag—Its Production, Processing, Characteristics, and Cementitious Properties. *J. Mater. Civ. Eng.* **2004**, *16*, 230–236. [CrossRef]
22. Hu, S.; Wang, H.; Zhang, G.; Ding, Q.J. Bonding and Abrasion Resistance of Geopolymeric Repair Material Made with Steel Slag. *Cem. Concr. Comp.* **2008**, *30*, 239–244. [CrossRef]
23. Tüfekçi, M.; Demirbaş, A.; Genc, H. Evaluation of Steel Furnace Slags as Cement Additives. *Cem. Concr. Res.* **1997**, *27*, 1713–1717. [CrossRef]
24. Wang, Q.; Yan, P. Hydration Properties of Basic Oxygen Furnace Steel Slag. *Constr. Build. Mater.* **2010**, *24*, 1134–1140. [CrossRef]
25. Zhao, J.; Yan, P.; Wang, D. Research on Mineral Characteristics of Converter Steel Slag and its Comprehensive Utilization of Internal and External Recycle. *J. Clean Prod.* **2017**, *156*, 50–61. [CrossRef]
26. Liu, S.; Li, L. Influence of Fineness on the Cementitious Properties of Steel Slag. *J. Therm Anal. Calorim.* **2014**, *117*, 629–634. [CrossRef]
27. Oluwasola, E.A.; Hainin, M.R.; Aziz, M.M.A.; Yaacob, H.; Warid, M.N.M. Potentials of Steel Slag and Copper Mine Tailings as Construction Materials. *Mater. Res. Innov.* **2014**, *18*, S6-250–S6-254. [CrossRef]
28. Pyzalski, M.; Dabek, J.; Adamczyk, A.; Brylewski, T. Physicochemical Study of the Self-Disintegration of Calcium Orthosilicate ($\beta \rightarrow \gamma$) in the Presence of the $C_{12}A_7$ Aluminate Phase. *Materials* **2021**, *14*, 6459. [CrossRef]
29. Chai, C.; Cheng, Y.C.; Zhang, Y.W.; Zhu, B.; Liu, H. Mechanical Properties of Crumb Rubber and Basalt Fiber Composite Modified Porous Asphalt Concrete with Steel Slag as Aggregate. *Polymers* **2020**, *12*, 2552. [CrossRef]
30. Wu, X.Q.; Zhu, H.; Hou, X.K.; Li, H.S. Study on Steel Slag and Fly Ash Composite Portland Cement. *Cem. Concr. Res.* **1999**, *29*, 1103–1106.

31. Gan, W.G.; Zhou, G.M. Comparison of Components and Structural Characteristics of Different Types of Steel Slag and Technical Characteristics of Steel Slag Powder. *Chin. Cem. Guide New Epoch.* **2022**, *28*, 1–5.
32. Guo, X.; Shi, H. Modification of SSP by Mineral Admixture and Chemical Activators to Utilize in Cement-based Materials. *Mater. Struct.* **2013**, *46*, 1265–1273. [CrossRef]
33. Muhmood, L.; Vitta, S.; Venkateswaran, D. Cementitious and Pozzolanic Behavior of Electric Arc Furnace Steel Slags. *Cem. Concr. Res.* **2009**, *39*, 102–109. [CrossRef]
34. Saly, F.; Guo, L.P.; Ma, R.; GU, C.P.; Sun, W. Properties of Steel Slag and Stainless Steel Slag as Cement Replacement Materials: A Comparative Study. *J. Wuhan. Univ. Technol.* **2018**, *33*, 1444–1451. [CrossRef]
35. Peng, Y.; Hu, S.; Ding, Q. Preparation of Reactive Powder Concrete Using Fly Ash and Steel Slag Powder. *J. Wuhan. Univ. Technol.* **2010**, *25*, 349–354. [CrossRef]
36. Liu, J.; Guo, R. Applications of SSP and Steel Slag Aggregate in Ultra-high Performance Concrete. *Adv. Civ. Eng.* **2018**, *2018*, 1–8.
37. Shi, Y.; Chen, H.; Wang, J.; Feng, Q.M. Preliminary Investigation on the Pozzolanic Activity of Superfine Steel Slag. *Constr. Build. Mater.* **2015**, *82*, 227–234. [CrossRef]
38. Zhang, S.; Niu, D.; Luo, D. Enhanced Hydration and Mechanical Properties of Cement-based Materials with Steel Slag Modified by Water Glass. *J. Mater. Res. Technol.* **2022**, *21*, 1830–1842. [CrossRef]
39. Xu, G.; He, X.; He, Y. Effect of Steel Slag and Granulated Blast-furnace Slag on the Mechanical Strength and Pore Structure of Cement Composites. *J. Wuhan. Univ. Technol.* **2018**, *33*, 1186–1192. [CrossRef]
40. Gan, L.; Wang, H.; Li, X.; Qi, Y.; Zhang, C. Strength Activity Index of Air Quenched Basic Oxygen Furnace Steel Slag. *J. Iron. Steel. Res. Int.* **2015**, *22*, 219–225. [CrossRef]
41. Zhang, T.; Yu, Q.; Wei, J.; Li, J. Investigation on Mechanical Properties, Durability and Micro-structural Development of Steel Slag Blended Cements. *J. Therm. Anal. Calorim.* **2012**, *110*, 633–639. [CrossRef]
42. Altun, I.A.; Yılmaz, İ. Study on Steel Furnace Slags with High MgO as Additive in Portland Cement. *Cem. Concr. Res.* **2002**, *32*, 1247–1249. [CrossRef]
43. Da Silva Magalhães, M.; Faleschini, F.; Pellegrino, C.; Pellegrino, C.; Brunelli, K. Influence of alkali addition on the setting and mechanical behavior of cement pastes and mortars with electric arc furnace dust. *Constr. Build. Mater.* **2019**, *214*, 413–419. [CrossRef]
44. Wang, Q.; Yan, P.; Feng, J. A Discussion on Improving Hydration Activity of Steel Slag by Altering its Mineral Compositions. *J. Hazard. Mater.* **2011**, *186*, 1070–1075. [CrossRef] [PubMed]
45. Wang, Q.; Yan, P.; Mi, G. Effect of Blended Steel Slag–GBFS Mineral Admixture on Hydration and Strength of Cement. *Constr. Build. Mater.* **2012**, *35*, 8–14. [CrossRef]
46. Wang, R. Influence of Steel Slag Powder on Concrete Performance. *Chin. J. Shandong Agric. Univ. (Nat. Sci. Ed.).* **2019**, *50*, 221–224.
47. Guan, S.P. *Research on the Active & Cementitious Capacity of Steel-Making Slag and its Concrete Properties*; China Wuhan University of Technology: Wuhan, China, 2008.
48. Li, Y.X. *Study on the Composition, Structure and Performance of Cement and Concrete with Steel-Making Slag Powder Mineral Additive*; China Building Materials Academy: Beijing, China, 2003.
49. Cai, Q.Y. Study on the Effect of Ground Steel Slag Powder on the Properties of Cement Concrete. *Chin. China Concr. Cem. Prod.* **2012**, *5*, 5–8.
50. Wang, Q.; Yang, J.; Yan, P. Cementitious Properties of Super-fine Steel Slag. *Powder Technol.* **2013**, *245*, 35–39. [CrossRef]
51. Ding, T.T.; Li, Q.H.; Cheng, H.D. Effect of Steel Slag on the Mechanical Properties and Durability of Concrete. *Chin. Bull. Chin. Ceram. Soc.* **2017**, *36*, 1723–1727.
52. Liu, P. *Study on the Compressive Strength and the Early Crack Resistance of Steel Slag Concrete*; China Xinjiang Agricultural University: Urumqi, China, 2014.
53. Luo, X.; Si, Y.; Gu, W. Effect of Silica Fume on Mechanical Properties of Concrete Incorporating SSP. *J. Wuhan Univ. Technol.* **2019**, *24*, 86–92. [CrossRef]
54. Sha, F.; Liu, P.; Ding, Y. Application Investigation of High-phosphorus Steel Slag in Cementitious Material and Ordinary Concrete. *J. Mater. Res. Technol.* **2021**, *11*, 2074–2091. [CrossRef]
55. Hussain, I.; Ali, B.; Rashid, M.U.; Amir, M.T.; Riaz, S.; Ali, A. Engineering Properties of Factory Manufactured Paving Blocks Utilizing Steel Slag as Cement Replacement. *Case. Stud. Constr. Mat.* **2021**, *15*, e00755. [CrossRef]
56. Li, Y.; Yao, Y.; Wang, L. Recycling of Industrial Waste and Performance of Steel Slag Green Concrete. *J. Cent. South Univ. T* **2009**, *16*, 768–773. [CrossRef]
57. Wang, Q.; Shi, M.X.; Yang, J. Influence of Classified Steel Slag with Particle Sizes Smaller than 20 μm on the Properties of Cement and Concrete. *Constr. Build. Mater.* **2016**, *123*, 601–610.
58. Wang, Q.; Wang, D.; Zhuang, S. The Soundness of Steel Slag with Different Free CaO and MgO Contents. *Constr. Build. Mater.* **2017**, *151*, 138–146. [CrossRef]
59. Song, K.; Liu, F.T. Research on the Influence of Steel Slag Powder, Slag Power, and Fly Ash on the Performance of Concrete. In Proceedings of the 2015 4th International Conference on Mechatronics, Materials, Chemistry and Computer Engineering, Xi'an, China, 12–13 December 2015; Atlantis Press: Amsterdam, The Netherlands, 2015.
60. Kourounis, S.; Tsivilis, S.; Tsakiridis, P.E.; Papadimitriou, G.D.; Tsibouki, Z. Properties and Hydration of Blended Cements with Steel-making Slag. *Cem. Concr. Res.* **2007**, *37*, 815–822. [CrossRef]

61. Young, J.F.; Berger, R.L.; Breese, J. Accelerated Curing of Compacted Calcium Silicate Mortars on Exposure to CO_2. *J. Am. Ceram. Soc.* **1974**, *57*, 394–397. [CrossRef]
62. Monshi, A.; Asgarani, M.K. Producing Portland Cement from Iron and Steel Slags and Limestone. *Cem. Concr. Res.* **1999**, *29*, 1373–1377. [CrossRef]
63. Dunstan, E.R. How Does Pozzolanic Reaction Make Concrete Green. In Proceedings of the 2011 World of Coal Ash (WOCA) Conference, Denver, CO, USA, 9–12 May 2011; pp. 1–14.
64. Telesca, A.; Marroccoli, M.; Pace, M.L.; Tomasulo, M.; Valenti, G.L.; Monteiro, P.J.M. A Hydration Study of Various Calcium Sulfoaluminate Cements. *Cement Concrete Comp.* **2014**, *53*, 224–232. [CrossRef]
65. Pelletier-Chaignat, L.; Winnefeld, F.; Lothenbach, B.; Jörg Müller, C. Beneficial Use of Limestone Filler with Calcium Sulphoaluminate Cement. *Constr. Build. Mater.* **2012**, *26*, 619–627. [CrossRef]
66. Wang, Y.L.; Hu, X.B.; Yao, Y.H.; Cui, S.P.; Wei, Q.; Hao, L.W. Research Progress of Slag Structure and Hydration Activity. In *Materials Science Forum*; Trans Tech Publications Ltd.: Stafa-Zurich, Switzerland, 2021; Volume 1035, pp. 972–979.
67. Hayet, C.; Ammar, N.; Nacira, S.; Khedidja, A.M. Mechanical Properties of Slag Sand Mixture used in Road Pavements. *Mag. Civ. Eng.* **2021**, *8*, 10806.
68. Erlin, B.; Jana, D. Forces of Hydration That Can Cause Havoc in Concrete. *Concr. Int.* **2003**, *25*, 51–57.
69. Li, Z.; Zhao, S.; Zhao, X.; He, T. Cementitious property modification of basic oxygen furnace steel slag. *Constr. Build. Mater.* **2013**, *48*, 575–579. [CrossRef]
70. Liao, L. *Study on the Gelation Properties of Composite of Steel Slag and Blast Furnace Slag, and the Reach of its Application for Marine Environment*; China Jinan University: Jinan, China, 2014.
71. Shi, Y. *Research on the Cementitious Properties of Superfine Steel Slag and the Utilization in Concrete*; Southwest University of Science and Technology: Mianyang, China, 2015.
72. Yang, J.W. *Influence of Steel Slag and Composite Mineral Admixture Containing Steel Slag on the Properties of Concrete*; China Tsinghua University: Beijing, China, 2013.
73. Song, K.Q. *Study on the Effect of Steel Slag Powder on the Performance of Road Concrete*; China Jinan of University: Jinan, China, 2016.
74. Wang, Q.; Li, M.Y.; Shi, M.X. Hydration Properties of Cement-Steel Slag-Ground Granulated Blast Furnace Slag Complex Binder. *Chin. J. Chin. Ceram. Soc.* **2014**, *42*, 629–634.
75. Liu, F. *Effect of Steel Slag Powder on Performance of Cement Based Materials*; China Wuhan University of Technology: Wuhan, China, 2015.
76. Li, Y.F.; Wang, L.; Lin, H. Workability and Mechanical Properties of Concrete with Steel Slag Powder. *Chin. Concrete* **2008**, *09*, 38–40.
77. Song, K.Q.; Liu, F.T.; Zhao, T.J.; Liu, L.Y. Influence of Steel Slag and Fly Ash on Concrete Characteristic and Its Hydration Mechanism. In Proceedings of the Energy, Environmental & Sustainable Ecosystem Development: International Conference on Energy, Environmental & Sustainable Ecosystem Development (EESED2015), Kunming, China, 26–28 August 2016.
78. Xu, C.; Ni, W.; Li, K.; Zhang, S.; Xu, D. Activation Mechanisms of Three Types of Industrial by-product Gypsums on Steel Slag–granulated Blast Furnace Slag-based Binders. *Constr. Build. Mater.* **2021**, *288*, 123111. [CrossRef]
79. Guilmeau, E.; Funahashi, R.; Mikami, M.; Chong, K.; Chateigner, D. Thermoelectric Properties–texture Relationship in Highly Oriented $Ca_3Co_4O_9$ Composites. *Appl. Phys. Lett.* **2004**, *85*, 1490–1492. [CrossRef]
80. Ren, Q. *Influence of Steel Slag Powder and Iron Oxide on the Performance of Concrete*; China Zhejiang University: Hangzhou, China, 2018.
81. Celik, I.B. The Effects of Particle Size Distribution and Surface Area upon Cement Strength Development. *Powder. Technol.* **2009**, *188*, 272–276. [CrossRef]
82. Li, Q.L.; Chen, M.Z.; Liu, F.; Wu, S.P.; Sang, Y. Effect of Superfine Blast Furnace Slag Powder on Properties of Cement-based Materials. *Mater. Res. Innov.* **2015**, *19*, S1-168–S1-171. [CrossRef]
83. Yang, X.J.; Zhou, H.Q.; Han, C.J.; Tang, Y.; He, C.M. Study on the Effect of Specific Surface Area and Content of Steel Slag on Cement Properties. *Chin. Dev. Guide Build. Mater.* **2013**, *11*, 42–45.
84. Ma, X.M.; Ni, W.; Liu, X. Experimental Study on Performance Optimization of Steel Slag Powder and Preparation of Non-Clinker Concrete. *Chin. Mater. Rev.* **2016**, *30*, 135–140.
85. Liu, F.; Chen, M.Z.; Li, F.Z.; Li, Q.L.; Wu, S.P.; Sang, Y. Effect of Ground Steel Slag Powder on Cement Properties. *Mater. Res. Innov.* **2015**, *19*, S1-150–S1-153. [CrossRef]
86. Singh, S.K.; Vashistha, P. Development of Newer Composite Cement Through Mechano-chemical Activation of Steel Slag. *Constr. Build. Mater.* **2021**, *268*, 121147. [CrossRef]
87. Hu, J. Comparison between the Effects of Superfine Steel Slag and Superfine Phosphorus Slag on the Long-term Performances and Durability of Concrete. *J. Therm. Anal. Calorim.* **2017**, *128*, 1251–1263. [CrossRef]
88. Wang, K.X.; Long, H.M.; Meng, Q.M.; Wei, R.F.; Zhang, H. Steel slag Cementitious Activity and Mechanism based on Physical Excitation. *Chin. Iron Steel.* **2018**, *53*, 82–86.
89. Zhao, F.C.; Ju, J.T.; Liao, J.L.; Kong, W.M.; Dang, Y.J. Analysis of Comprehensive Utilization and Basic Properties of Converter Slag processed. *Chin. J. Iron Steel Res.* **2013**, *25*, 23–28.
90. Wang, Z. *Research on Steel Slag Used as Cement Mixture*; China Hebei University of Engineering: Handan, China, 2020.
91. Davidovits, J. Geopolymers and Geopolymeric Materials. *J. Therm. Anal Calorim.* **1989**, *35*, 429–441. [CrossRef]
92. Pacheco-Torgal, F.; Castro-Gomes, J.; Jalali, S. Alkali-activated Binders: A Review: Part 1. Historical Background, Terminology, Reaction Mechanisms and Hydration Products. *Constr. Build. Mater.* **2008**, *22*, 1305–1314. [CrossRef]

93. Provis, J.L.; Palomo, A.; Shi, C. Advances in Understanding Alkali-activated Materials. *Cem. Concr. Res.* **2015**, *78*, 110–125. [CrossRef]
94. Palomo, A.; Grutzeck, M.W.; Blanco, M.T. Alkali-activated Fly Ashes: A cement for the Future. *Cem. Concr. Res.* **1999**, *29*, 1323–1329. [CrossRef]
95. Wang, Y. *Study on Active Excitation of Steel Slag and Application of Building Materials*; China Anhui University of Science and Technology: Hefei, China, 2018.
96. Dong, L.R. *Preparation of Low-Clinker Cement with Steel Slag and Application in Concrete*; China Inner Mongolia University of Science & Technology: Baotou, China, 2020.
97. Ionescu, D.; Meadowcroft, T.R.; Barr, P.V. Early-age Hydration Kinetics of Steel Slags. *Adv. Cem. Res.* **2001**, *13*, 21–30. [CrossRef]
98. Cerulli, T.; Pistolesi, C.; Maltese, C.; Salvioni, D. Durability of Traditional Plasters with Respect to Blast Furnace Slag-based Plaster. *Cem. Concr. Res.* **2003**, *33*, 1375–1383. [CrossRef]
99. Hu, S.G.; Wei, J.X.; Ding, Q.J. Study on the Excitation Mechanism of Water Glass on Steel Slag Cement. *Chin. Cem. Eng.* **2001**, *5*, 4–6+52.
100. Feldman, R.F.; Carette, G.G.; Malhotra, V.M. Studies on Mechanics of Development of Physical and Mechanical Properties of High-volume Fly Ash-cement Pastes. *Cement. Concr. Comp.* **1990**, *12*, 245–251. [CrossRef]
101. Wu, F.H.; Wang, Y.; Zhang, C.S.; Yang, F.L.; Hu, Z.C.; Sheng, D. Effect of Activator on Gelling Activity and Microstructure of Steel Slag. *Chin. Concr.* **2019**, *12*, 99–102.
102. Cui, X.W.; Di, Y.Q.; Xu, C.Y. Preparation of High-Performance Concrete Mixed with Steel Slag Powder and Tailings. *Chin. China Concr. Cem. Prod.* **2016**, *9*, 78–81.
103. Liu, H.; Shen, Y.C.; Deng, Z.; Zhou, H.W.; Jin, Q.; Zhang, Z.Z. Effect of Mineral Admixtures and Steam Curing Methods on The Mechanical Properties of Steel Slag Concrete with Pipe Segments. *Chin. China Concr. Cem. Prod.* **2018**, *6*, 35–38.
104. Zhang, Z.Z.; Jin, Q.; He, J.C.; Liu, H.; Li, H.G. Different Ways of Curing Effect on the Properties of Steel Slag Concrete Compressive Strength. *Chin. Fly Ash Compr. Util.* **2017**, *2*, 12–16.
105. Zhang, Z.Z.; Feng, Y.; Jin, Q.; He, J.C.; Liu, H. Mechanical Properties of Steel-Slag Concrete Contained Different Mineral Admixtures. *Chin. Concr.* **2017**, *11*, 110–113.
106. Wang, F.H. *The Experimental Research on Physical Mechanical Properties and Frost Resistance of Mineral Admixture to Steel Slag Concrete*; China Xinjiang Agricultural University: Urumqi, China, 2016.
107. Han, F.H.; Zhang, Z.Q.; Wang, D.M.; Yan, P.Y. Hydration Heat Evolution and Kinetics of Blended Cement Containing Steel Slag at Different Temperatures. *Thermochim Acta* **2015**, *605*, 43–51. [CrossRef]
108. Zhuang, S.Y.; Wang, Q. Inhibition Mechanisms of Steel Slag on the Early-Age Hydration of Cement. *Cem. Concr. Res.* **2021**, *140*, 106283. [CrossRef]

Disclaimer/Publisher's Note: The statements, opinions and data contained in all publications are solely those of the individual author(s) and contributor(s) and not of MDPI and/or the editor(s). MDPI and/or the editor(s) disclaim responsibility for any injury to people or property resulting from any ideas, methods, instructions or products referred to in the content.